NJC

Accepted Manuscript

This is an *Accepted Manuscript*, which has been through the Royal Society of Chemistry peer review process and has been accepted for publication.

Accepted Manuscripts are published online shortly after acceptance, before technical editing, formatting and proof reading. Using this free service, authors can make their results available to the community, in citable form, before we publish the edited article. We will replace this *Accepted Manuscript* with the edited and formatted *Advance Article* as soon as it is available.

You can find more information about *Accepted Manuscripts* in the Information for Authors.

Please note that technical editing may introduce minor changes to the text and/or graphics, which may alter content. The journal's standard Terms & Conditions and the Ethical guidelines still apply. In no event shall the Royal Society of Chemistry be held responsible for any errors or omissions in this *Accepted Manuscript* or any consequences arising from the use of any information it contains.

ROYAL SOCIETY OF CHEMISTRY

www.rsc.org/njc

Facile synthesis of ultrathin worm-like Au nanowires for highly active SERS substrates

Ai-Jun Wang, Jing-Jing Lv, Dan-Ling Zhou, Xuexiang Weng, Su-Fang Qin, Jiu-Ju Feng*

College of Geography and Environmental Science, College of Chemistry and Life Science, Zhejiang Normal University, Jinhua 321004, China

**Corresponding author: jjfeng@zjnu.cn (JJF), Tel./Fax: +86 579 82282269.*

Abstract

In this report, ultrathin worm-like Au nanowires were constructed with the assistance of *L*-glutamic acid as a structure directing agent and a weak stabilizing agent. The morphology of the Au products was found to be strongly dependant on the experimental parameters such as *L*-glutamic acid and its amount, as well as the reaction temperature. This synthesis was a seedless process, without using any template, surfactant, or toxic organic agent. Besides, the as-prepared Au nanowires were applied to facilely fabricate porous Au films with controllable thickness via simple gravity settling. Thus-formed Au films showed high surface enhanced Raman scattering (SERS) enhancement, using 4-mercaptobenzoic acid as a model probe. It might employ as a promising candidate for SERS sensing. This strategy provides an environmental friendly way for preparation of various metal nanostructures with novel morphologies and useful applications.

Keywords: Worm-like Au nanowires; porous Au film; *L*-glutamic acid; surface enhanced Raman scattering; 4-mercaptobenzoic acid

1 Introduction

Surface-enhanced Raman scattering (SERS) is a powerful analytical tool in determining chemical information for molecules on metallic substrates.[1-5] A variety of Raman-active Au hierarchical nanostructures have been prepared for generating SERS signals with high-magnitude enhancement, along with good stability and reproducibility.[6-8] It demonstrates that tremendous enhancement of SERS signals comes from electromagnetic enhancement at the "hot spots" in interstitial voids, intersections of metal nanoparticles, and high radii of curvature of the metal structures.[9] The electromagnetic field would be greatly enhanced in hierarchical Au structures composed of numerous small Au nanoparticles by self-organization, which is benefit to obtain high quality Raman active Au substrates.

The Au nanowires have enhanced catalytic activity, high electric conductivity, and unique optical property,[10,11] unlike individual Au nanoparticles and their bulk counterparts. To date, many methods have been developed for preparation of Au nanowires, including chemical vapor deposition,[12] wet-chemical synthesis, photochemical synthesis,[13] electroless deposition,[14,15] and electrochemical deposition.[16-18]

Au nanowires are usually formed from assembly of tiny Au nanoparticles by oriented attachment via hydrogen-bonding, S-Au bond, metal-ion coordination, dipole–dipole and π–π interactions, and steric hindrance.[19] Thus-formed Au nanowires were sometimes involved in a time-consuming assembly process that is separated from the synthesis step, in which some organic or poisonous agents are

inevitably poison the sample and further limit their potential applications in catalysis and sensors. For example, the *L*-cysteine coated Au dendrites seriously affected their catalytic performance for ethanol oxidation.[20]

Most importantly, direct deposition of hierarchical Au nanostructures on substrates plays an important role for integrating Au artificial materials into functional devices. Now, many attempts have been made for design and construction of Au films such as self–assembly at interface,[21,22] lithographically,[23] and electrochemical method.[24,25] For instance, Liu and coworkers fabricated Au nanoporous films from the network-like Au nanowires,[26] and make it used as a SERS-active substrate.[27]

In this report, ultrathin worm-like Au nanostructures were facilely prepared by a one-step seedless synthetic approach at 0 °C, with the help of *L*-glutamic acid as a structure directing agent and a weak stabilizing agent. Meanwhile, through the sedimentation of the as-prepared Au nanowires, porous Au films were constructed and examined as SERS-active substrates, using 4-mercaptobenzoic acid (4-MBA) as a model probe.

2 Experimental

2.1 Chemicals

$HAuCl_4$, *L*-glutamic acid, and 4-mercaptobenzoic acid (4-MBA) were purchased from Shanghai Aladdin Chemical Reagent Company (Shanghai, China). All the other chemicals were analytical grade and used without further treatment. All aqueous solutions were prepared with twice distilled water.

2.2 Instruments

UV-vis spectra of the samples were recorded on a Lambda 950 UV-vis spectrometer (PerkinElmer, USA). The crystal structures were examined by X–ray diffraction (XRD) analysis on a Rigaku Dmax–2000 diffractometer with Cu Kα radiation (Bruker Co., Germany). The morphology was characterized by field emission scanning electron microscopy (SEM, JEOL JSM-6390LV). The transmission electron microscopy (TEM) analysis was performed at an accelerating voltage of 200 kV, and Cu grids were used as substrates. The selected-area electron diffraction (SAED) pattern was recorded on a JEOL JEM-2100F TEM operating at an accelerating voltage of 200 kV. Raman spectroscopy analysis was conducted on a microscopic confocal Raman spectrometer employing a 633 nm laser beam and a charge-coupled detector (CCD) with 4 cm^{-1} resolution (Renishaw PLC, England, R-1000 series).

2.3 Synthesis of the ultrathin worm-like Au nanowires

For typical synthesis of the ultrathin worm-like Au nanowires, 100 μL of 24.3 mM $HAuCl_4$ was put into 10 mL of 10 mM *L*-glutamic acid and stirred under ice bath (0 °C). The mixed solution immediately turned blue upon the addition of 100 μL of freshly-prepared 0.1 M $NaBH_4$.

Control experiments were preformed for preparation of the Au products by varying the reaction temperature from 0 to 90 ℃, while the other experimental conditions were kept constant.

2.4 Construction of the porous Au films and Raman measurements

The porous Au film was prepared based on simple gravity settling.[27] The freshly prepared colloidal solution of the Au nanowires was put into a clean bottle with desired height (0.5, 1.0, 2.0, 3.0, and 4.0 cm), followed by putting the clean quartz foils on the bottle bottom. The solution remained static until the colloidal Au nanowires were completely deposited on the quartz foils. Afterwards, the upper colorless solution was carefully removed with a pipettor. The resulting Au films with different thickness were thoroughly washed with ethanol and dried in air.

Next, the Au films were immersed into the 4-MBA ethanolic solution with different concentrations (2×10^{-5} M, 5×10^{-5} M, 1×10^{-4} M, 2×10^{-4} M, and 5×10^{-4} M) for 12 h in dark. When the films were immersed into 4-MBA solution, 4-MBA molecules would be self-assembled on the surfaces of the porous Au films via the interactions between Au and the mercapto groups of 4-MBA as well as Benzenethiol[28]. Then, the 4-MBA ethanolic solution was moved away, followed by thoroughly washing the Au films with water and absolute ethanol to remove free 4-MBA molecules and dried at room temperature. For comparison, a bare quartz foil covered with 4-MBA molecules was prepared by directly dropping 100 μL of a 4-MBA ethanolic solution (0.01 M) under the same conditions. Raman measurements were performed on a Renishaw Raman system model 1000 spectrometer equipped with CCD detector, performed with a He/Ne laser at a wavelength of 633 nm. The laser power at the sample position was 1.25 mW, with an acquisition time of 10 s for all spectra. The spectra were obtained by focusing a 1-2 μm laser spot on the sample

using a 20 ×objective lens. All spectra were normalized for the same integration time. The size of the Au films was large enough for observation with the confocal microscope of the Raman spectrometer. Therefore, the laser spot was focused on the top of the Au films to record the spectra and each spectrum was repeated at least 3 times under the identical conditions.

3 Results and discussion

3.1 Characterization of the worm-like Au nanowires

Ultrathin worm-like Au nanowires were synthesized using *L*-glutamic acid as a structure directing agent and a weak stabilizing agent via a one-step, template-free and surfactant-free route. Figure 1 shows the typical Au product synthesized from a $HAuCl_4$ solution containing 10.0 mM *L*-glutamic acid under ice bath (0 °C). The product contains many ultrathin nanowires with an average length of several micrometers (Figure 1A) and diameter of 15 nm (Figure 1B). Most of them are enclosed as loops, resulting into the formation of worm-like nanostructures interconnected by nanowires. This observation is in good agreement with the SEM results (Figure 2), in which uniform, loose, and worm-like Au nanostructures are observed. Additionally, the SAED pattern indicates polycrystalline nature of the worm-like Au nanowires (inset in Figure 1B), similar to our previous work of flower-like Au nanochains.[19]

HRTEM image (Figure 1C) provides a deep insight on the joint region of the worm-like Au nanowires (taken from the blue square area in Figure 1B), confirming

that the nanowires are fused together by crystal growth, rather than linking by amorphous structures or foreign molecules. The clear lattice fringes are detected in different regions with the same d-spacing value of 0.238 nm, corresponding to the (111) planes of face-centered cubic (fcc) Au,[29] although each one owns different orientation. This value is well consistent with the branched and flower-like Au nanochains,[30] suggesting that the worm-like Au nanowires are preferentially growing along the (111) directions. Furthermore, the orientations of the lattice fringes regularly change along the nanowires, confirming polycrystalline nature of the Au nanowires, as demonstrated by the above SAED test.

As shown in Figure 1D, XRD analysis indicates high crystallinity of the worm-like Au nanowires, in which the representative diffraction peaks are consistent with the (111), (200), (220), (311), and (222) planes of the fcc Au (JCPDS 04-0784, a = 4.0786 Å). This observation is matched well with our previous work.[29,31,32] Furthermore, the peak intensity ratio of the (111) planes relative to the (200) and (220) planes are 2.73 and 4.57, respectively. These values are similar to the flower-like Au nanochains (3.29 and 4.62, respectively)[19] and Au dendrites in the cysteine solution (3.1 and 5.9, respectively),[20] but larger than the common spherical Au nanoparticles (1.9 and 3.1, respectively, JCPDS 04-0784). These results reveal that the as-prepared Au nanocrystals are preferentially growing along the (111) planes.

To understand the formation mechanism of the worm-like Au nanowires, control experiments are performed by varying the concentration of *L*-glutamic acid (Figure 3). Decreasing the concentration of *L*-glutamic acid (e.g. 5.0 mM, Figure 3B) yields

similar Au nanowires with extended lengths and decreased diameters. And short Au nanorods are obtained as the concentration of *L*-glutamic acid is dropped to 2.5 mM (Figure 3A), coalesced by several small Au particles. Alternatively, increasing the concentrations of *L*-glutamic acid to 50 mM (Figure 3C) and 100 mM (Figure 3D) produces similar Au nanowires with shorter lengths and larger diameters. These results mean that the concentration of *L*-glutamic acid has a key role in the formation of the Au nanowires. The results are similar to the previous report for synthesis of Au nanochains using amino acids as a capping agent.[33]

Figure 4 shows the TEM images of the series products prepared at different reaction temperature. Similar Au nanowires with shortened lengths and decreased diameters are emerged by increasing the temperature up to 50 °C (Figure 4A). This observation is agreed well with the corresponding UV-vis spectra (Figure 5). The colloidal Au nanowires show two characteristic absorption peaks at 510~530 nm and 710~800 nm, which are ascribed to the transverse and longitudinal absorptions, respectively.[34] Furthermore, the broadened peak at 710~800 nm is consistent with the formation of the anisotropic nature of Au nanoparticles in the aqueous solution.[35] These findings are similar to the Au nanostructures in the literature.[35]

With the increase of the temperature to 90 °C, short nanowires or nanorods are observed (Figure 4B), as supported by the UV-vis behavior where the absorption peak at 520 nm is gradually declined, accompanied with the increase of the peak at 715 nm (Figure 5, curve a-d). In their work, increasing the temperature improves the quality of the products. These results indicate that low temperature is desirable for synthesis

of the worm-like Au nanowires, which is different from the Au nanochains prepared at the air/water interface[36] and Pd ultrathin nanowires obtained by the polyol method.[37]

The formation mechanism of the worm-like Au nanowires in the presence of *L*-glutamic acid can be directed by oriented attachment based on the dipole–dipole interactions.[38] At the very early stage, a large number of Au atoms are quickly produced upon the addition of $NaBH_4$, owing to the extremely fast reduction rate between $AuCl_4^-$ ions and $NaBH_4$. The adjacent *L*-glutamic acid molecules will rapidly adsorbed onto the surface of Au atoms. The *L*-glutamic acid capped gold atoms have strong dipole–dipole interactions due to the zwitterionic nature of *L*-glutamic acid,[33] which would be the dominant driving force for fusion of nanoparticles into nanowires. When the dipole–dipole interactions were stronger than those of thermal energy and electrostatic repulsion between the colloidal particles, causing the linear assembly of colloidal particles with an intrinsic or induced dipole moments.[33] This oriented attachment mechanism are consistent with the anisotropic structures of Au nanowires and nanochains in the literature.[19, 33, 36]

Compared with the previous reports,[10,11] this strategy is simple, green, and rapid, without using any seed, template, surfactant, or toxic organic agent. It provides a green way to use biomolecules as a structure directing agent and weak stabilizing agent for fabrication of other metal nanostructures. Moreover, this simple one-step wet-chemical route is easy to synthesis on a large-scale.

3.2 SERS measurements

The porous Au films with different thickness were fabricated by the sedimentation of the colloidal Au nanowires for SERS measurements, using 4-MBA as model molecules.[39,40] Figure 6 provides the corresponding SERS spectra of 4-MBA. There are two strong and sharp peaks located at 1590 and 1080 cm^{-1}, respectively, which are assigned to the ring-breathing modes.[41] Meanwhile, several relatively weaker vibrational bonds are also detected, such as a bending mode at 1173 cm^{-1} ($\delta_{(CH)}$) and a stretching mode at 1375 cm^{-1} ($\nu_{s(COO-)}$). For this work, the ring-breathing mode located at 1590 cm^{-1} is selected as an instructive peak, which is the most intense of the Raman modes sensitive to the thickness of the Au film. It is found that Raman signals are greatly enhanced by increasing the film thickness, owing to high spatial density of hot spots available.

Herein, the surface enhancement factor (EF) was determined using the following expression.[42]

$$EF = (I_{SERS}/I_{Raman})/(N_{ads}/N_{bulk})$$

where N_{bulk} and N_{ads} represent the number of 4-MBA molecules in the bulk and samples adsorbed on the Raman active substrates, respectively. I_{SERS} is the intensity of the ring-breathing mode 1590 cm^{-1} ($\nu_{(C-C)}$) and I_{Raman} is the intensity of the same mode in the Raman spectrum.

N_{ads} is calculated based on the following equation: [43,44]

$$N_{ads} = RA/\sigma$$

where R is the roughness factor of the surface, defined as the ratio of real surface to the geometric surface, which can be obtained from the electrochemical experiments.[45]

A is the area of the focal spot of the laser in our system. It is known that the diameter of the laser spot is 2 μm and thus A is 3.14×10^{-8} cm^2. Meanwhile, σ is the area occupied by a molecule of adsorbent at monolayer coverage. According to the previous reports,[46,47] the bonding density of 4-MBA molecules in a self-assembled monolayer is ca. 0.5 nmol cm^{-2}. Therefore, σ is 2.0×10^9 cm^2 mol^{-1}.

Figure S1 (Supporting information) shows the typical cyclic voltammograms (CVs) of the Au nanowires modified electrode in 0.5 M H_2SO_4, which displays the characteristic peaks of Au. The electrochemically active surface area (EASA) can be estimated from Coulombic integration of the enhanced cathodic peak current at 0.89 V.[45] The electrochemically active surface area is 0.349 cm^2. We also obtained the real area of the bare GCE with a value of 0.062 cm^2, based on the CVs in 1.0 mM $K_3[Fe(CN)_6]$ at different scan rates.[48] As a result, the roughness factor (R) is 5.63, and the N_{ads} is 8.84×10^{-17} mol. On the other hand, the sampling volume was obtained based on the area of the laser spot (ca. 2 μm in diameter) and the penetration depth (ca. 2 μm) of the focused beam (Figure S2), with the 4-MBA density of 1.5 g cm^{-3} and its molecular weight of 154.19 g mol^{-1}. The number of 4-MBA molecules (N_{bulk}) was calculated to be 3.68×10^{10} (i.e. 6.11×10^{-14} mol), which are efficiently excited by the laser beam.[47]

As displayed in Figure S2 (Supporting information), the SERS intensity significantly increases after the absorption of 4-MBA on the porous Au film (curve a), compared with those on the quartz plate (curve b). The EF is calculated to be 2.7×10^4, using the SERS intensity at 1590 cm^{-1}, indicating high SERS enhancement of the

porous Au film. This result is consistent with the previous reports.[49] As illustrated in Figure 1, the worm-like Au nanowires with many enclosed loops are interconnected together and form porous networks. The as-prepared Au nanowires were further used to fabricate thickness-controlled porous Au films by a simple gravity settling method. The porous Au films have high surface areas, with the R of up to 5.63. As shown in Figure 2, the porous Au films provide sharp tips and valleys, and "hot spots" for localized near-field enhancements, leading to the enlarged EF of the porous Au films.

Impressively, the Raman intensities are almost unchanged for the deposition of the Au films by the Au products obtained at different temperature, while other conditions were the same (Figure 6). These observations indicate that the reaction temperature for preparing Au nanostructures is not the critical factor for the SERS enhancement, which is totally different from the thickness-controlled experiments that are essential to the Raman signals (Figure 7), possibly owing to the similar porous structures of the deposited Au films.

As shown in Figure 8, the SERS intensities increase with the increase of the 4-MBA concentrations. The intensities have good linear relationship with the concentrations of 4-MBA in the range from 2×10^{-5} to 5×10^{-4} M, with the correlation coefficient of 0.9972 (Figure 8B) and a detection limit of 7.4 μM (S/N=3), using the SERS intensity at 1590 cm^{-1}.

4 Conclusions

In this work, we facilely prepared ultrathin worm-like Au nanowires with the

assistance of *L*-glutamic acid as a structure directing and a weak stabilizing agent via a one-step, template-free, and surfactant-free route. The presence of *L*-glutamic acid and its amount, as well as the reaction temperature, were found to be the key factors during the synthesis process, and their growth mechanism was discussed. The Au nanowires were extended for the construction of porous Au film with control thickness via the simple gravity settling. The as-prepared Au film displayed excellent SERS enhancement with Raman enhancement factors up to 2.7×10^4 and a detection limit of 7.4 μM for 4-mercaptobenzoic acid. This simple and rapid strategy provides Raman active substrates with high-quality for SERS sensing.

Acknowledgements

This work was financially supported by the NSFC (Nos. 21175118 and 21275130), Zhejiang Province university young academic leaders of academic climbing project (No. pd2013055) and Natural Science Foundation of Zhejiang Province (No. LQ12B05002).

References

1 H. Jia, J. Zeng, J. An, W. Xu and B. Zhao, *J. Colloid Interf. Sci.*, **2005**, 292, 455-461.

2 X. Li, W. Xu, J. Zhang, H. Jia, B. Yang, B. Zhao, B. Li and Y. Ozaki, *Langmuir*, **2004**, 20, 1298-1304.

3 M. Fleischmann, P. J. Hendra and A. J. McQuillan, *Chem. Phys. Lett.*, **1974**, 26,

163-166.

4 D. L. Jeanmaire and R. P. Van Duyne, *J. Electroanal. Chem. Interf. Electrochem.*, **1977**, 84, 1-20.

5 M. G. Albrecht and J. A. Creighton, *J. Am. Chem. Soc.*, **1977**, 99, 5215-5217.

6 Y. Zhang, S. Sun, D. Deng, X. Song, B. Ding and Z. Yang, *CrystEngComm*, **2012**, 14, 656-662.

7 B. K. Jena and C. R. Raj, *Chem. Mater.*, **2008**, 20, 3546-3548.

8 L. Rodriguez-Lorenzo, R.A. Alvarez-Puebla, F.J. Garcia de Abajo and L.M. Liz-Marzan, *J. Phys. Chem. C*, **2010**, 114, 7336-7340.

9 H. Zhu, M. Du, M. Zou, C. Xu and Y. Fu, *Dalton Trans.*, **2012**, 41, 10465-10471.

10 C. M. Cobley, J. Chen, E. C. Cho, L. V. Wang and Y. Xia, *Chem. Soc. Rev.*, **2011**, 40, 44-56.

11 J.Y. Xiao and L.M. Qi, *Nanoscale*, **2011**, 3, 1383-1396.

12 H. Araki, A. Fukuoka, Y. Sakamoto, S. Inagaki, N. Sugimoto, Y. Fukushima and M. Ichikawa, *J. Mol. Catal. A: Chem.* **2003**, 199, 95-102.

13 W.-B. Zhao, J.-J. Zhu and H.-Y. Chen, *J. Cryst. Growth*, **2003**, 258, 176-180.

14 M. Wirtz and C. R. Martin, *Adv. Mater.*, **2003**, 15, 455-458.

15 J. Gu, J. Shi, L. Xiong, H. Chen, L. Li and M. Ruan, *Solid State Sci.*, **2004**, 6, 747-752.

16 X. Y. Zhang, L. D. Zhang, Y. Lei, L. X. Zhao and Y. Q. Mao, *J. Mater. Chem.*, **2001**, 11, 1732-1734.

17 M. Tian, J. Wang, J. Kurtz, T. E. Mallouk and M. H. W. Chan, *Nano Lett.*, **2003**, 3,

919-923.

18 P. Forrer, F. Schlottig, H. Siegenthaler and M. Textor, *J. Appl. Electrochem.*, **2000**, 30, 533-541.

19 A.-J. Wang, S.-F. Qin, D.-L. Zhou, L.-Y. Cai, J.-R. Chen and J.-J. Feng, *RSC Adv.*, **2013**, 3, 14766-14773.

20 T.-H. Lin, C.-W. Lin, H.-H. Liu, J.-T. Sheu and W.-H. Hung, *Chem. Commun.*, **2011**, 47, 2044-2046.

21 R. Zhang, M. Hummelgard and H. Olin, *Phys. Status Solidi A*, **2012**, 209, 519-523.

22 S.-C. Yang, X.-W. Wan, Y.-T. Ji, L.-Q. Wang, X.-P. Song, B.-J. Ding and Z.-M. Yang, *CrystEngComm*, **2010**, 12, 3291-3295.

23 M. T. Carlson, A. J. Green, A. Khan and H. H. Richardson, *J. Phys. Chem. C*, **2012**, 116, 8798-8803.

24 M.-S. Hsu, Y.-L. Chen, C.-Y. Lee and H.-T. Chiu, *ACS Appl. Mater. Interfaces*, **2012**, 4, 5570-5575.

25 S. Cherevko and C.-H. Chung, *Sens. Actuators B: Chem*, **2009**, 142, 216-223.

26 R. Liu, J.-F. Liu, X.-X. Zhou and G.-B. Jiang, *Anal. Chem.*, **2011**, 83, 3668-3674.

27 R. Liu, J.-F. Liu, X.-X. Zhou, M.-T. Sun and G.-B. Jiang, *Anal. Chem.*, **2011**, 83, 9131-9137.

28 L.-J. Wan, M. Terashima, H. Noda and M. Osawa, *J. Phys. Chem. B*, **2000**, 104, 3563-3569.

29 J.-J. Feng, A.-Q. Li, Z. Lei and A.-J. Wang, *ACS App.l Mater. Interfaces*, **2012**, 4, 2570-2576.

30 D.-F. Zhang, L.-Y. Niu, L. Jiang, P.-G. Yin, L.-D. Sun, H. Zhang, R. Zhang, L. Guo and C.-H. Yan, *J. Phys. Chem. C*, **2008**, 112, 16011-16016.

31 A.-J. Wang, Y.-F. Li, M. Wen, G. Yang, J.-J. Feng, J. Yang and H.-Y. Wang, *New J. Chem.*, **2012**, 36, 2286-2291.

32 Z.-Y. Lv, A.-Q. Li, Y. Fei, Z. Li, J.-R. Chen, A.-J. Wang and J.-J. Feng, in *Electrochim. Acta*, 2013, 136-144.

33 L. Polavarapu and Q.-H. Xu, *Nanotechnology*, **2008**, 19, 75601-75606.

34 S. Lin, M. Li, E. Dujardin, C. Girard and S. Mann, *Adv. Mater.*, **2005**, 17, 2553-2559.

35 T. Huang, F. Meng and L. Qi, *Langmuir*, **2009**, 26, 7582-7589.

36 H. Jia, X. Bai and L. Zheng, *CrystEngComm*, **2012**, 14, 2920-2925.

37 Y. Wang, S.-I. Choi, X. Zhao, S. Xie, H.-C. Peng, M. Chi, C. Z. Huang and Y. Xia, *Adv. Funct. Mater.*, **2014**, 24, 131-139.

38 R. L. Penn and J. F. Banfield, *Science*, **1998**, 281, 969-971

39 S. J. Lee and M. Moskovits, *Nano Lett.*, **2011**, 11, 145-150.

40 X. Zhang, Z. Lu, D. Sim, S. Li, Y. Feng, J. Ma, H. Chen, F. Boey, H. H. Hng and Q. Yan, *Chem.-Eur. J.*, **2011**, 17, 13386-13390.

41 C. E. Talley, L. Jusinski, C. W. Hollars, S. M. Lane and T. Huser, *Anal. Chem.*, **2004**, 76, 7064-7068.

42 E. C. Le Ru, E. Blackie, M. Meyer and P. G. Etchegoin, *J. Phys. Chem. C*, **2007**, 111, 13794-13803.

43 W. B. Cai, B. Ren, X. Q. Li, C. X. She, F. M. Liu, X. W. Cai and Z. Q. Tian, *Surf.*

Sci., **1998**, 406, 9-22.

44 H. Jia, J. Zeng, W. Song, J. An and B. Zhao, *Thin Solid Films*, **2006**, 496, 281-287.

45 J.-J. Feng, Z.-Y. Lv, S.-F. Qin, A.-Q. Li, Y. Fei and A.-J. Wang, *Electrochim. Acta*, **2013**, 102, 312-318.

46 C. J. Orendorff, A. Gole, T. K. Sau and C. J. Murphy, *Anal. Chem.*, **2005**, 77, 3261-3266.

47 L. Xia, Y. Jia, G. Liu, Z. Yang, X. Chen, H. Zhang and M. Sun, *J. Raman Spectr.*, **2010**, 41, 398-405.

48 H. Ju, S. Liu, B. Ge, F. Lisdat and F. W. Scheller, *Electroanalysis*, **2002**, 14, 141-147.

49 Y. Huang and D.-H. Kim, *Nanoscale*, **2012**, 4, 6312-6317.

Captions

Figure 1. Low (A) and middle (B) TEM images, and X-ray diffraction pattern (D) of the worm-like Au nanowires. The corresponding HRTEM image (C) marked in image (B). Inset shows the associated SAED patterns.

Figure 2. Typical SEM image of the porous film prepared with the worm-like Au nanowires.

Figure 3. TEM images of the Au products obtained using different concentrations of *L*-glutamic acid: 2.5 mM (A), 5 mM (B), 50 mM (C), and 100 mM (D).

Figure 4. TEM images of the Au products obtained at different temperature: 50 ℃ (A) and 90 ℃ (B).

Figure 5. UV-vis spectra of the colloidal Au solution obtained at different temperature: 0 ℃ (curve a), 25 ℃ (curve b), 50 ℃ (curve c), 70 ℃ (curve d), and 90 ℃ (curve e).

Figure 6. SERS spectra of 4-MBA on the porous Au nanofilms with different thickness.

Figure 7. SERS spectra of 4-MBA on the porous Au nanofilms deposited by the Au nanowires at different reaction temperature.

Figure 8. SERS spectra of the Au films after immersing into the 4-MBA ethanolic solution with different concentrations.

Figures

Figure 1

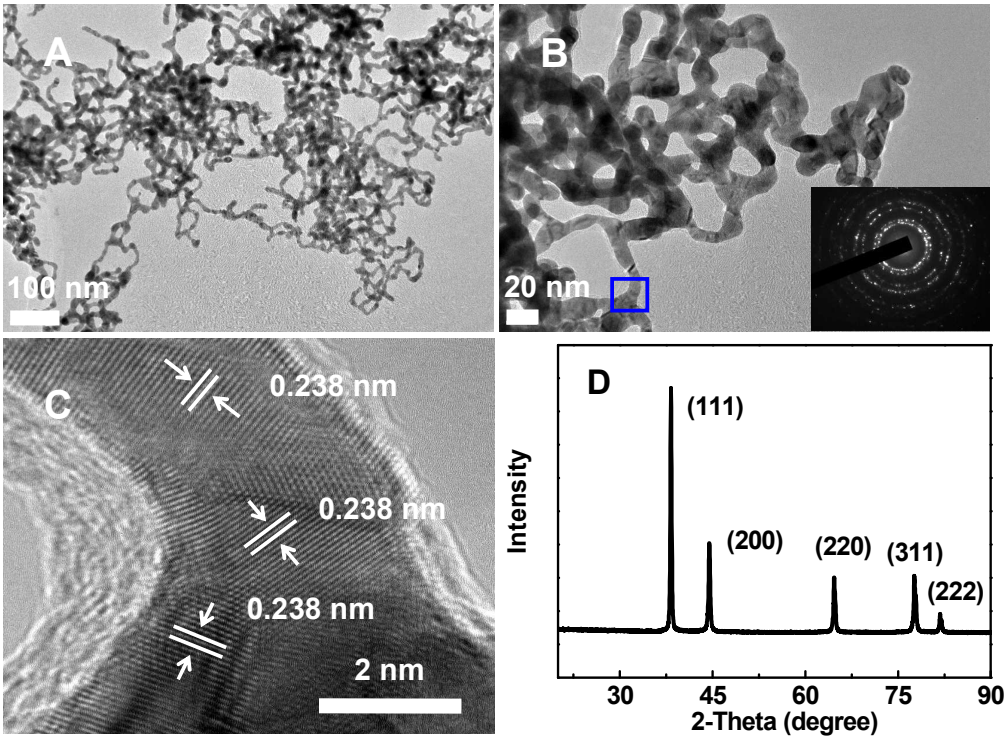

Figure 2

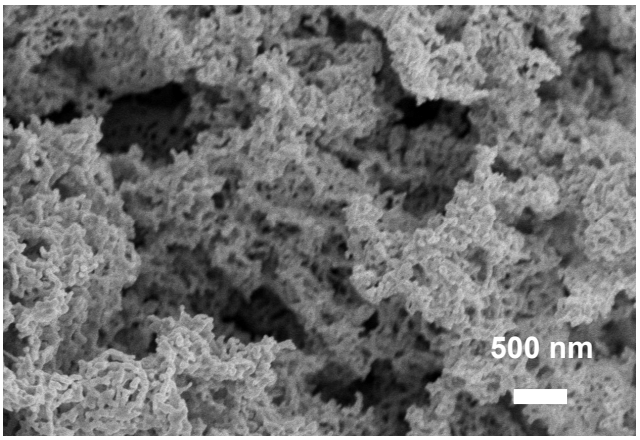

Figure 3

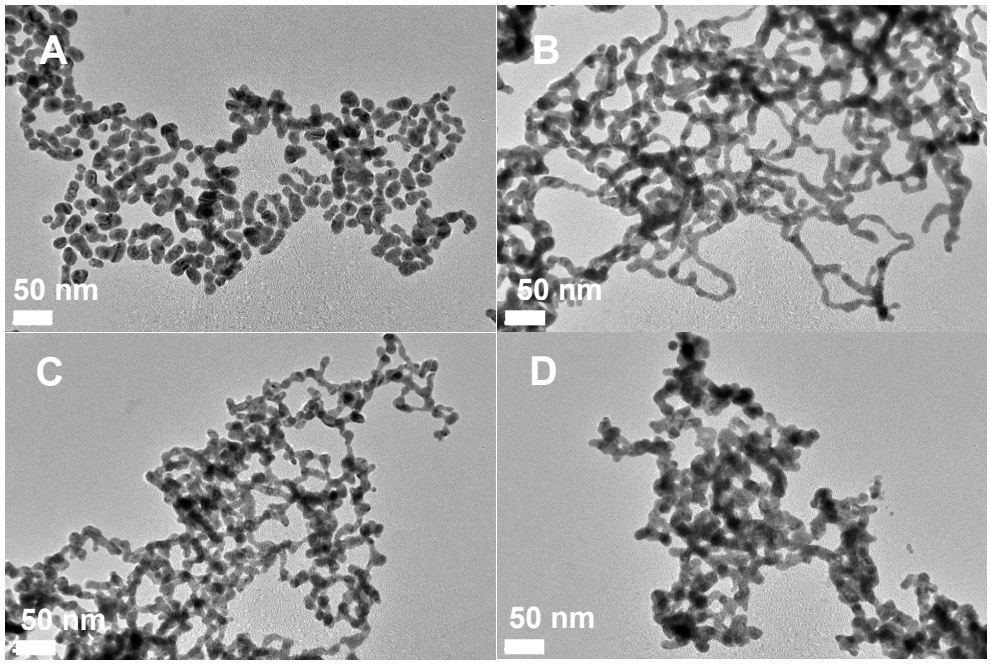

Figure 4

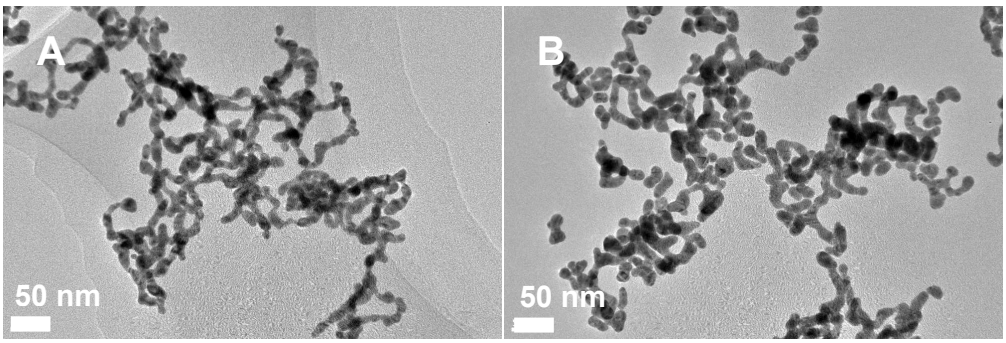

Figure 5

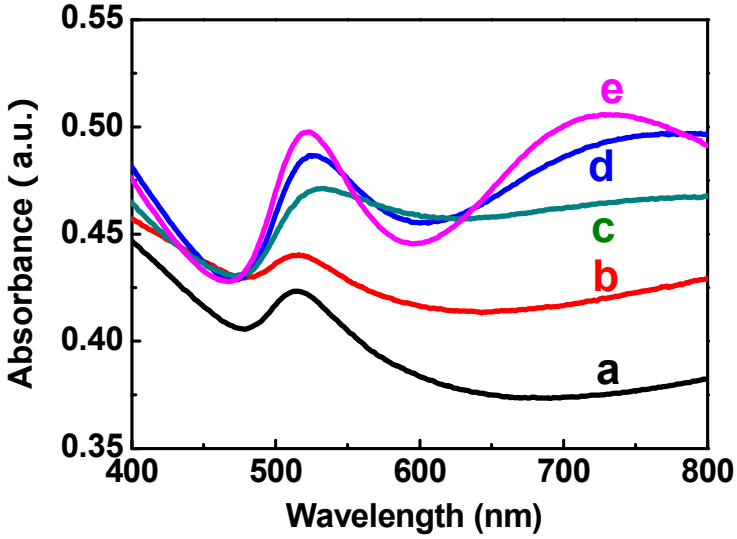

Figure 6

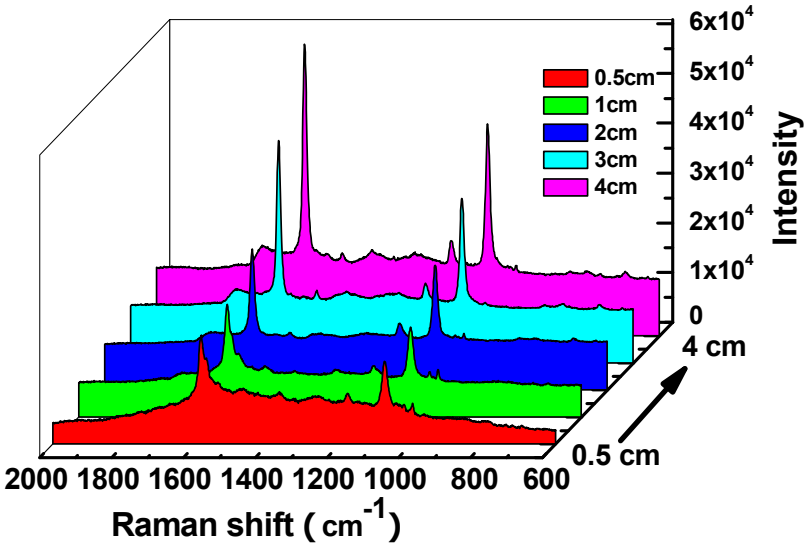

Figure 7

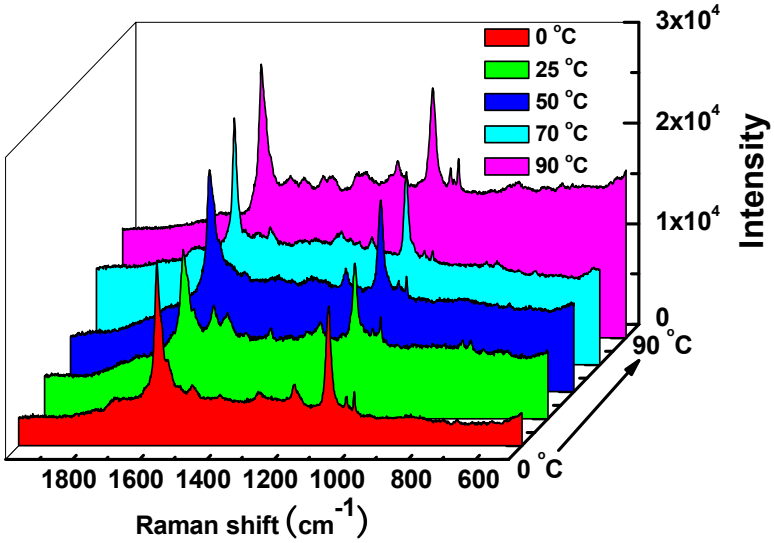

Figure 8